Bubble-Free Membrane Gas Transfer in Mammalian Cell Culture Bioreactors: An Alternative to Conventional Bubble Sparging

By: David Guthary[1], Patrick Montoya[2], Shiva Abdolrahimi[1]
[1]Keck Graduate Institute, [2]MedArray, Inc.

Specific Aims

The objective of this study was to evaluate the feasibility of replacing conventional bubble sparging for cell culture aeration with bubble-free gas transfer using a silicone membrane gas exchanger. Feasibility was assessed based on oxygen transfer performance and key indicators of CHO cell culture performance, including cell viability, viable cell density, and metabolite profiles during fed-batch operation.
This study also establishes practical start-up and operating guidelines for implementing bubble-free membrane gas transfer in mammalian cell culture bioreactors. Collectively, the findings demonstrate the potential of membrane-based, bubble-free gas transfer as an alternative aeration strategy for upstream bioprocessing.

Summary of Results

This study demonstrated that a 0.5-m² silicone membrane gas exchanger provided sufficient oxygen transfer to meet the metabolic demands of a 1.8-L CHO cell culture while maintaining effective dissolved oxygen (DO) control without the need for bubble sparging. Under the conditions evaluated, the membrane gas exchanger achieved oxygen transfer performance comparable, or greater than, that of conventional bubble sparging. These findings indicate that recirculation of the cell suspension through the pump and membrane gas exchanger did not adversely affect cell growth or viability and suggest that the associated hydrodynamic stresses were well tolerated by the CHO cells under the operating conditions evaluated.

1. Introduction

Maintaining dissolved oxygen (DO) within an appropriate operating range is essential for the successful intensification and scale-up of mammalian cell culture bioreactors. Intensified processes achieve high volumetric productivity by increasing viable cell density and sustaining culture performance over extended durations. These gains are accompanied by increased volumetric oxygen uptake rates, which place greater demands on bioreactor oxygen-transfer capacity.

Stirred-tank bioreactors commonly use agitation and bubble sparging to provide oxygen. Although Chinese hamster ovary (CHO) cell lines generally tolerate the hydrodynamic conditions encountered in properly designed bioreactors, excessive local energy dissipation and bubble-associated phenomena can adversely affect cell viability and productivity [1–3]. In particular, cell attachment to gas–liquid interfaces and bubble rupture at the culture surface can expose cells to damaging stresses. Increasing agitation speed or gas flow to satisfy the oxygen demand of high-density cultures may also increase foaming and the requirement for antifoam agents. Therefore, oxygen-delivery strategies for intensified CHO processes must provide adequate oxygen transfer while limiting potentially detrimental hydrodynamic and bubble-associated effects.

Bubble-free oxygenation through a nonporous silicone membrane provides an alternative to direct gas sparging. Oxygen diffuses through the gas-permeable membrane into the culture medium without forming bubbles, thereby eliminating bubble-rupture-associated stresses and reducing foam formation. The oxygen-transfer capacity of this approach depends on the membrane properties and surface area, the oxygen partial-pressure driving force, and liquid-side mass-transfer resistance. In the present study, we characterize the oxygen-transfer performance of a silicone membrane gas exchanger and evaluate its ability to fully support

or supplement the oxygen requirements associated with mammalian cell culture. The results establish the operating conditions and oxygen-transfer capacity of this bubble-free system and assess its potential application to intensified cell culture processes.

2. Methods

2.1. System Configuration

The system configuration is illustrated in Figure 1. The system components included:

Bioreactor vessel (Chemglass, CLS-1380-P01)
Pump (Levitronix DCP-200.3)
Pressure transducer (PendoTECH single use pressure sensor 3/8", PRESS-N-038)
Gas exchanger (PermSelect PDMSXA-5000 LD)
Clamp-on flowmeter (Keyence FD-H22F Clamp-On Flow Sensor)
Digital Control Unit -DCU with MFC's (Applikon ez-Control)
Dissolved CO_2 probe (InPro 5000i/220)

The system components were interconnected using silicone tubing (3/8" ID x 5/8" OD). The length of all tubing segments was kept as short as possible to minimize resistance to flow. This ensured that the pump speed was kept as low as possible to minimize cell damage while maintaining the required gas exchanger flow.

The components were connected as follows: the bottom spout of the bioreactor vessel was connected to the pump inlet. The pump outlet was connected to the gas exchanger inlet. The pressure transducer was placed in the tubing section between the pump outlet and the gas exchanger inlet. Changes in inlet pressure were monitored as an indicator of increasing flow resistance or potential fouling of the gas exchanger. The cell culture fluid exiting the gas exchanger was returned to the bioreactor through a port in the vessel headplate. A clamp-on flowmeter was installed in the return line between the gas exchanger outlet and the bioreactor to monitor the recirculation flow rate.

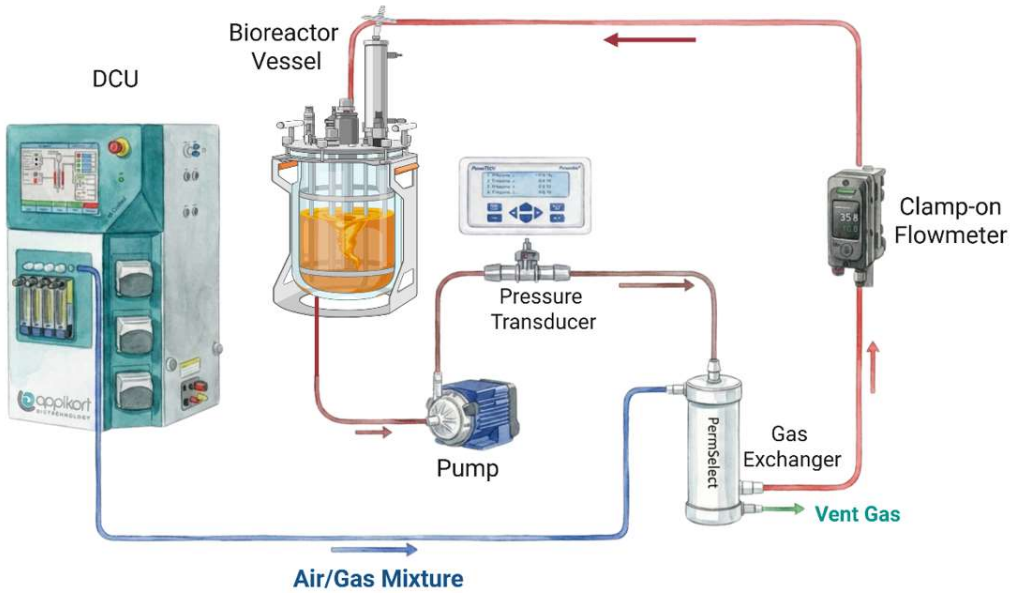

Figure 1. Schematic of the bubble-free membrane gas transfer system for CHO cell culture.

For gas delivery, the air/gas mixture supplied by the DCU was initially directed to the bioreactor sparger during process start-up and subsequently redirected to the gas inlet of the membrane gas exchanger for bubble-free oxygenation. The gas exiting the membrane gas exchanger was vented to the atmosphere.

2.2. Bioreactor and Cell Culture Conditions

CHO cells were cultured in a 1.8-L working volume of EX-CELL® Advanced CHO Fed-Batch Medium in a stirred-tank bioreactor. The culture was inoculated at a viable cell density (VCD) of 0.78×10^6 cells/mL with an initial viability of 99.3%. The medium was supplemented with L-glutamine and penicillin-streptomycin to final concentrations of 4 mM and 1% (v/v), respectively.

The culture temperature was maintained at 37 °C using a heating jacket with feedback from the bioreactor temperature probe. Agitation was maintained at 140 rpm using a standard Rushton impeller positioned approximately three-quarters of the distance down the impeller shaft. The culture pH was maintained within a range of 7.0–7.4.

Samples were collected once daily to determine viable cell density, cell viability, and extracellular metabolite concentrations. VCD and viability were measured using a Vi-CELL Cell Viability Analyzer, while metabolite concentrations were measured using a Cedex® Bio Analyzer.

2.3. Dissolved Oxygen Control and Aeration Strategy

The dissolved oxygen (DO) setpoint was maintained at 40% throughout the cell culture run. The culture was initially operated using conventional bubble sparging while the external membrane gas exchanger recirculation loop remained clamped, preventing circulation of the cell suspension through the centrifugal pump and membrane gas exchanger. During this phase, DO was automatically controlled by the DCU using a constant air flow with supplemental oxygen supplied as required to maintain the 40% DO setpoint.

On day 4, when the culture reached a VCD of 5.8×10^6 cells/mL, oxygenation was transitioned from conventional bubble sparging to bubble-free membrane gas transfer. Bubble sparging was discontinued, the DCU gas supply was redirected to the gas inlet of the membrane gas exchanger, and the external cell culture recirculation loop was opened. The centrifugal pump was then initiated to circulate the cell suspension from the bioreactor through the membrane gas exchanger and back to the vessel.

During membrane-based oxygenation, the DCU continued to regulate the gas supply using constant air flow with supplemental oxygen supplied as required to maintain the 40% DO setpoint. The liquid recirculation flow rate through the membrane gas exchanger was adjusted manually using the centrifugal pump.

3. Results and Discussion

3.1. Cell Growth and Oxygenation Performance

Figures 2–8 summarize the cell growth, metabolite, and process data obtained from daily sampling throughout the 14-day bioreactor run. Figure 2 shows the viable cell density (VCD) profile and the transition from conventional bubble sparging to bubble-free membrane gas transfer on day 4.

During the initial bubble-sparging phase, the culture exhibited the expected exponential growth profile for this CHO cell line. By day 3, air sparging alone was no longer sufficient to maintain the DO setpoint of

40%, and supplemental O_2 was automatically introduced by the DCU. On day 4, immediately prior to transitioning to membrane-based oxygenation, the sparger was supplied with a constant air flow of 70 mL/min and supplemental O_2 at flow rates of up to 125 mL/min.

On day 4, conventional bubble sparging was discontinued, and oxygenation was transitioned to the membrane gas exchanger. Following the transition, the 40% DO setpoint was initially maintained with only 20 mL/min of air supplied to the gas exchanger, demonstrating effective oxygen transfer through the membrane at the prevailing cell density and oxygen demand. As the VCD and associated oxygen demand increased on day 5, the air flow to the gas exchanger was increased to 70 mL/min, and supplemental O_2 was introduced, reaching a maximum flow rate of 35 mL/min.

Importantly, the transition from bubble sparging to membrane-based oxygenation did not interrupt the cell growth trajectory. VCD continued to increase following the switch, reaching a peak of 23.3×10^6 cells/mL on day 9. This peak VCD was approximately 16% higher than the historical maximum achieved at the facility for this CHO cell line using conventional bubble sparging, indicating that circulation through the pump and membrane gas exchanger did not adversely affect cell growth under the conditions evaluated.

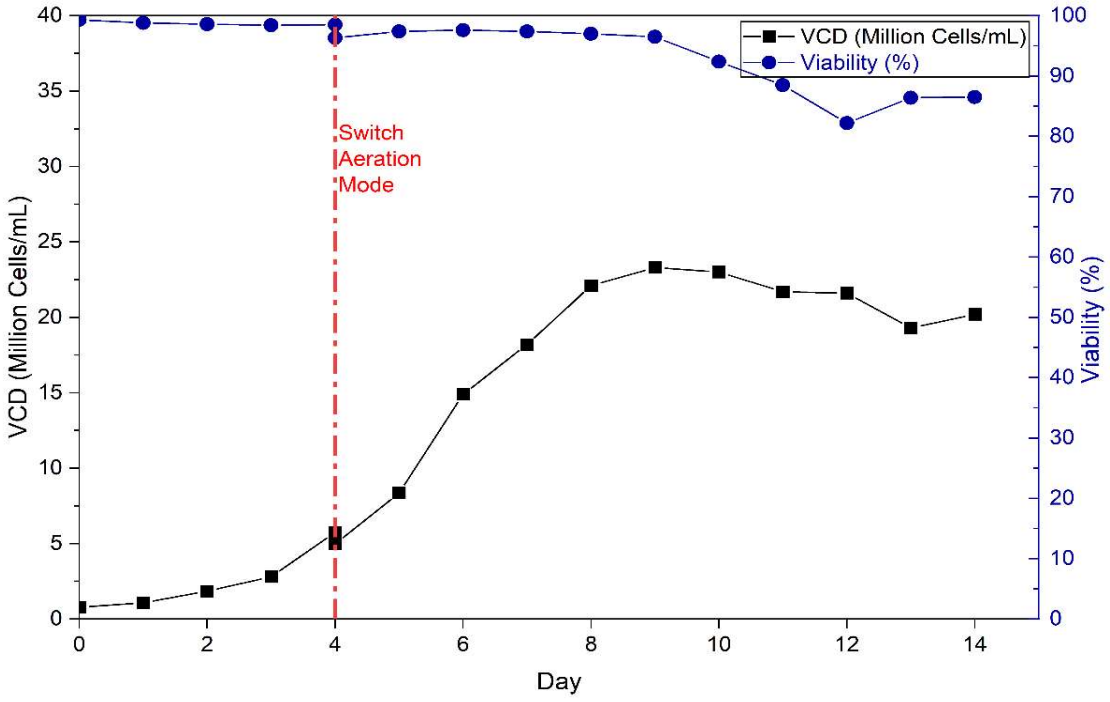

Figure 2. Viable cell density and cell viability during the cell culture process. Viable cell density (VCD; black squares) and cell viability (blue circles) are shown over the 14-day culture period.

As Shown in Figure 2, the cell viability remained above 96% through day 10, after which it began to decline, consistent with the expected culture viability profile observed with conventional bubble sparging. The maintenance of high cell viability following the transition to membrane-based oxygenation indicates that recirculation of the cell suspension through the centrifugal pump and membrane gas exchanger did not adversely affect cell viability under the conditions evaluated

As shown in Figure 3, the initial cell culture recirculation flow rate through the membrane gas exchanger was set at 0.8 L/min. This initial flow rate was established empirically to maintain the target dissolved

oxygen (DO) level of 40%. Gas flow to the membrane gas exchanger was automatically regulated by the DCU, as described above. As viable cell density increased, resulting in greater cellular oxygen demand, the recirculation flow rate was manually increased as needed to maintain the 40% DO setpoint. Figure 4 shows the corresponding changes in recirculation flow rate over the course of the culture.

Figure 3 shows the centrifugal pump speed (rpm) required to achieve the corresponding recirculation flow rates through the membrane gas exchanger.

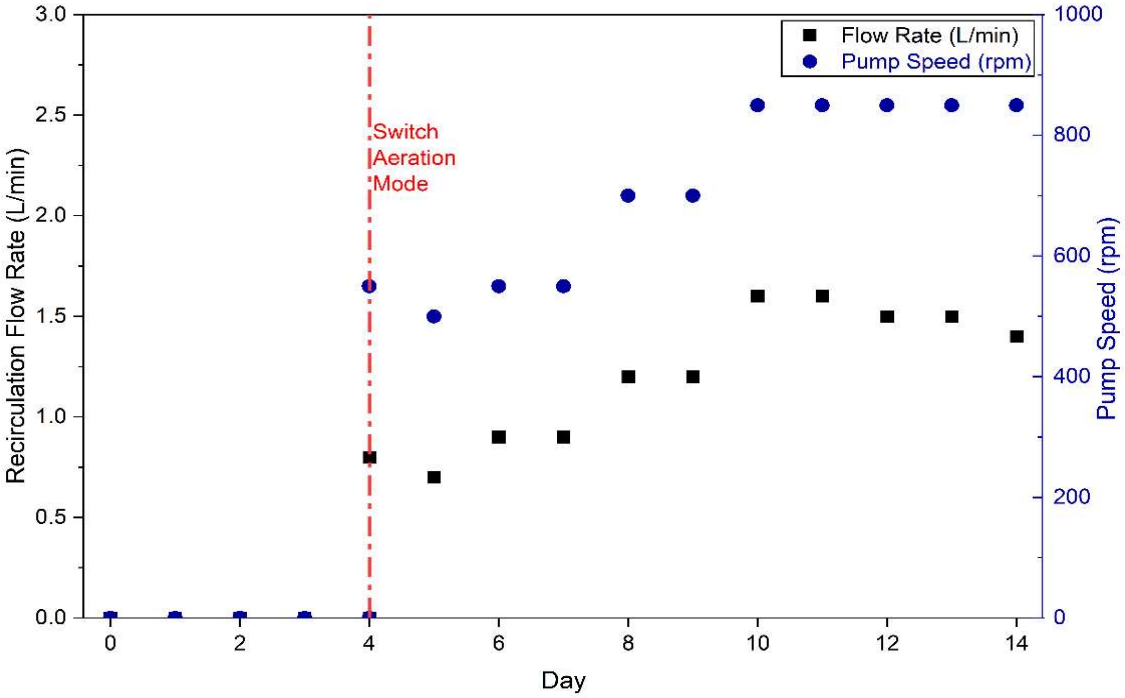

Figure 3. Recirculation flow rate and pump speed during bubble-free aeration. Recirculation flow rate (black squares) and pump speed (blue circles) are shown over the 14-day culture period. The red dashed vertical line at Day 4 indicates the transition to bubble-free aeration.

3.2. Nutrient Utilization and Metabolic Profiles

The extracellular metabolite profiles demonstrate changes in nutrient utilization and metabolite production throughout the culture (Figure 4). Glucose decreased during periods of cellular consumption, while the observed increases in glucose concentration corresponded to feed additions during the culture (Figure 4a). Thus, fluctuations in glucose primarily reflect the combined effects of cellular consumption and feeding. Glutamine decreased rapidly from approximately 4.1 mmol/L at inoculation to ~0.4 mmol/L by Day 4 and remained relatively low thereafter (Figure 4c), consistent with continued glutamine utilization.

Lactate accumulated during the initial growth phase, increasing from approximately 0.1 g/L to a maximum of ~1.9 g/L around Day 6, followed by a decline during the later culture period (Figure 4b). This pattern suggests a transition from net lactate production toward reduced production and/or lactate consumption as the culture progressed. Ammonia increased during early culture, reaching approximately 5 mmol/L around Day 5, followed by a transient decrease and subsequent accumulation to approximately 4.5–5.2 mmol/L during the later stages (Figure 4d). Overall, the transition to bubble-free aeration on Day 4 did not coincide

with an abrupt adverse shift in the extracellular metabolite profiles (Figure 4a–d); nutrient utilization and metabolic activity continued following the aeration-mode transition.

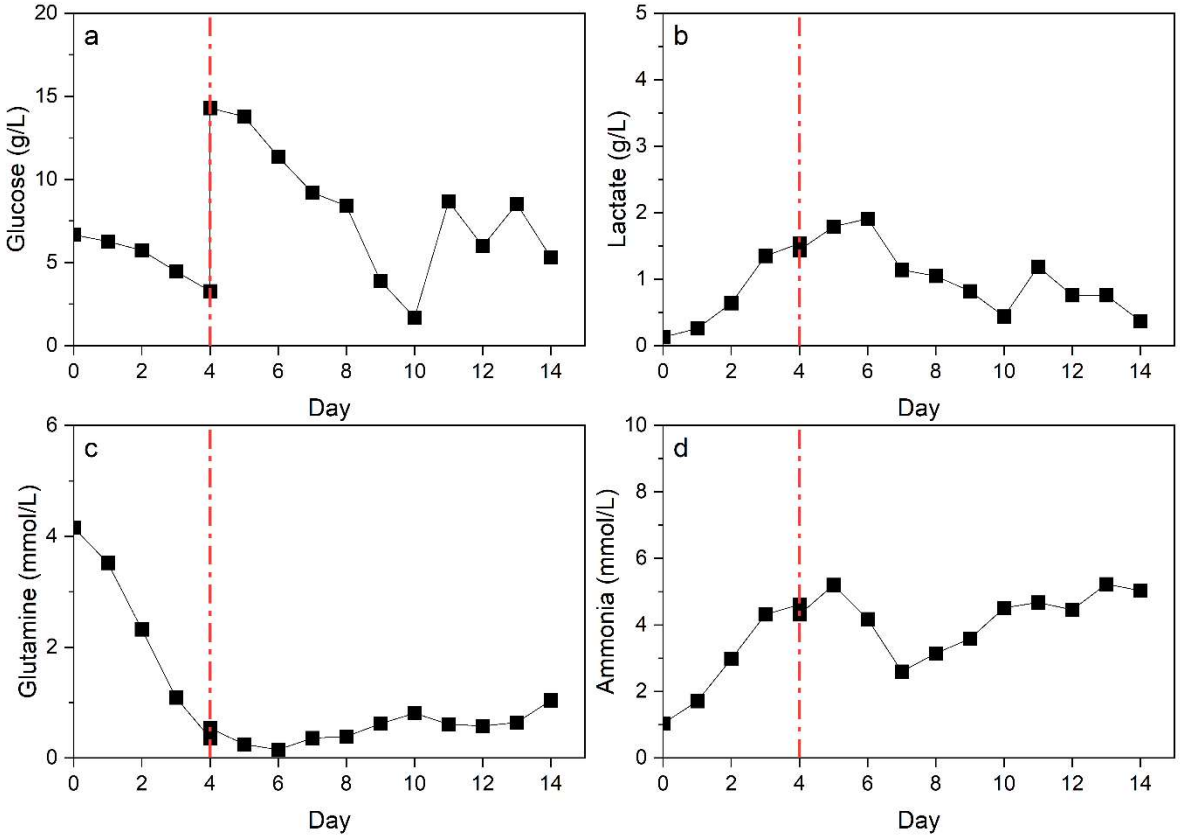

Figure 4. Extracellular metabolite profiles during the cell culture process. Time-course profiles of (a) glucose, (b) lactate, (c) glutamine, and (d) ammonia concentrations over the 14-day culture period. The red dashed vertical line at Day 4 indicates the initiation of bubble-free sparging.

3.3. Dissolved CO_2 Dynamics

Dissolved CO_2 (dCO_2) was monitored throughout the culture to evaluate CO_2 accumulation and removal following the transition from conventional bubble sparging to bubble-free aeration using a membrane gas exchanger on Day 4 (Figure 5). Prior to the aeration-mode transition, dCO_2 fluctuated between approximately 5% and 12%. Following implementation of bubble-free aeration, dCO_2 initially remained below 10% but subsequently increased to approximately 14–15% by Days 7–8 and remained elevated during the high-cell-density phase, reaching a maximum of approximately 17.5% on Day 13. The increase in dCO_2 coincided with continued cell expansion, with VCD increasing after Day 4 and reaching approximately 23 million cells/mL by Day 9 (Figure 2). Despite the increase in dCO_2, positive cell growth was therefore maintained during bubble-free aeration. In addition, pH measurements above the target setpoint suggested that CO_2 removal through the membrane gas exchanger was also happening, necessitating supplemental CO_2 addition to the bioreactor headspace to maintain the desired pH. However, because dCO_2 increased concurrently with culture age and biomass, the observed dCO_2 profile alone does not establish that CO_2 clearance was more effective with bubble-free aeration than with conventional bubble sparging.

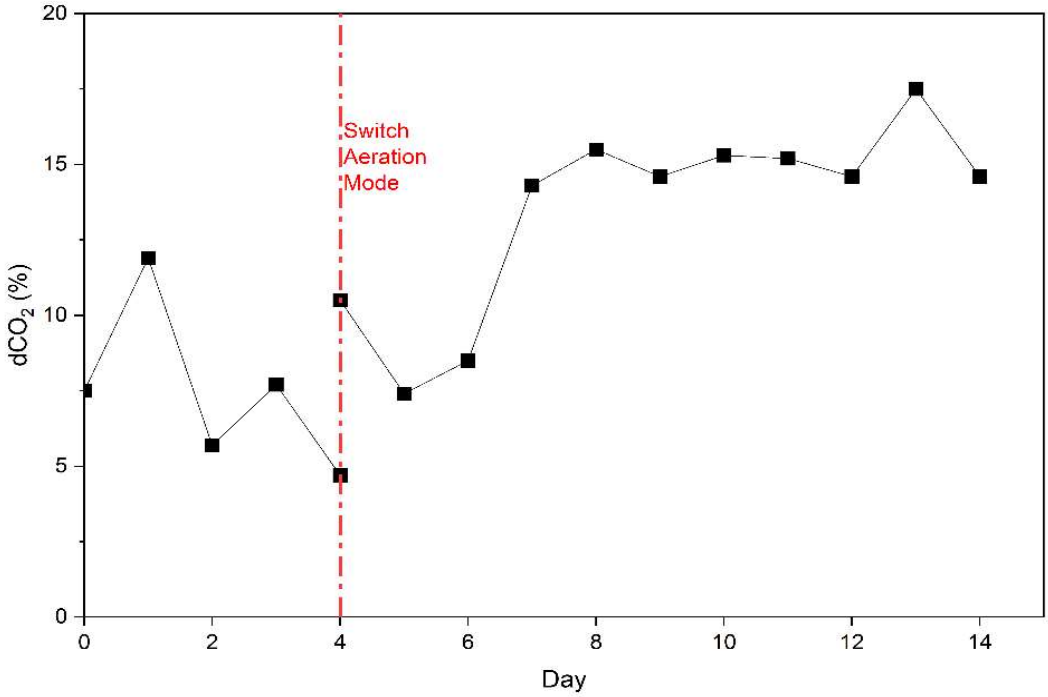

Figure 5. Dissolved carbon dioxide during the cell culture process. The concentration of CO_2 in the bioreactor (dCO_2) is shown over the 14-day culture period. The red dashed vertical line at Day 4 indicates the transition to bubble-free aeration.

To further assess the relationship between dCO_2 and cell growth, the day-to-day relative VCD increase was plotted against the corresponding dCO_2 concentration (Figure 6). A clear inverse relationship was observed, with the largest relative VCD increases (~50–105%) occurring at lower dCO_2 concentrations of approximately 5–8%, while relative cell growth progressively decreased as dCO_2 increased. Notably, under bubble-free aeration, positive VCD increases were maintained at dCO_2 concentrations of approximately 14–15.5%, indicating that the culture continued to expand despite relatively elevated dCO_2. At higher dCO_2 concentrations (~15–18%), the relative VCD change approached zero and eventually became negative, consistent with the transition toward stationary and death phases observed in the VCD profile (Figure 2). Taken together, Figures 2, 5, and 6 indicate that increasing dCO_2 was associated with decreasing relative cell growth as the culture progressed; however, the data do not demonstrate a direct inhibitory effect of elevated dCO_2. Because dCO_2, cell density, culture age, and growth phase changed concurrently.

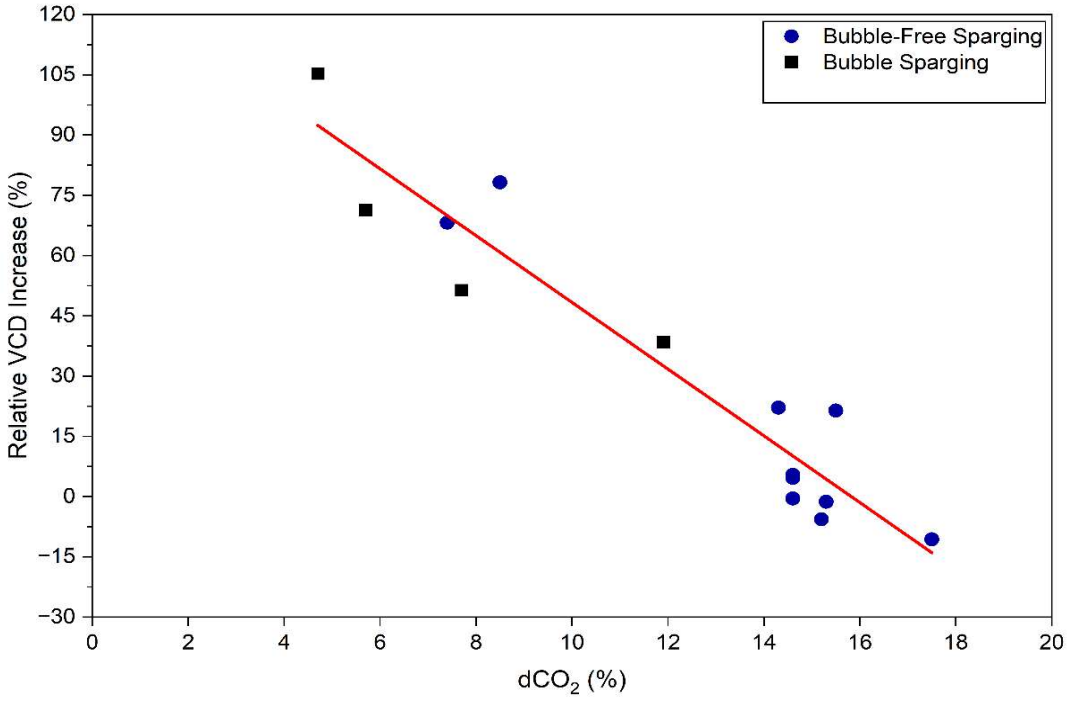

Figure 6. Relationship between dissolved CO_2 and relative VCD increase under bubble and bubble-free sparging conditions. Relative VCD increase between consecutive sampling days is plotted as a function of dCO_2 concentration. Black squares represent measurements during bubble sparging, while blue circles represent measurements during bubble-free sparging. The red line represents the overall linear regression across the data.

References

[1] Michaels JD, Mallik AK, Papoutsakis ET. Sparging and agitation-induced injury of cultured animals cells: Do cell-to-bubble interactions in the bulk liquid injure cells? Biotechnol Bioeng. 1996 Aug 20;51(4):399-409. doi: 10.1002/(SICI)1097-0290(19960820)51:4<399::AID-BIT3>3.0.CO;2-D. PMID: 18629792.

[2] Pani A. Apostolidis, Alice Tseng, Marie-Eve Koziol, Michael J. Betenbaugh, Barbara Chiang, Investigation of low viability in sparged bioreactor CHO cell cultures points to variability in the Pluronic F-68 shear protecting component of cell culture media, Biochemical Engineering Journal, Volume 98, 2015, Pages 10-17.

[3] Walls, P.L.L., McRae, O., Natarajan, V. et al. Quantifying the potential for bursting bubbles to damage suspended cells. Sci Rep 7, 15102, 2017.